Engineering Science & Technology
http://ojs.wiserpub.com/index.php/EST/

UNIVERSAL WISER PUBLISHER

Research Article

Design of Wideband Dielectric Near-Field Lens for Medical Applications in Tumor Treatment

Behrooz Haghshenas-Kashani*, Mohammad-Ali Damavandi, Mohammad Khalaj-Amirhosseini

Department of Electrical Engineering, Iran University of Science and Technology, Tehran, Iran
Email: b_haghshenas95@alumni.iust.ac.ir

Received: 28 March 2022; **Revised:** 17 June 2022; **Accepted:** 4 July 2022

Abstract: This paper presents a dielectric near-field lens for hyperthermia applications in tumor cell destruction, unlike the previous methods that used microstrip near-field lenses. Dielectric lenses benefit from operating in a wideband frequency range, low profile, and no surface current generated on them. The proposed dielectric lens is divided into 13 symmetric regions and each region comprises exclusive dielectric constants that contribute to microwave energy aggregation in the tumor area. The microwave energy accumulation leads to tumor cell destruction after therapeutic purpose temperature elevation during a defined time. The proposed near-field lens is designed for both superficial and deep-seated tumors. Specific Absorption Rate (SAR) and Effective Treatment Area (ETA) principles are used to analyze the lens effect on electromagnetic wave distribution on the phantom simulated human body. Based on the achieved SAR and ETA distribution on the biological phantom at 2.4 GHz, the proposed lens for superficial tumors demonstrated effective performance in focusing electromagnetic waves on the desired focal point.

***Keywords*:** antenna design, dielectric near-field lens, hyperthermia application, microwave energy accumulation, superficial tumor treatment, deep-seated tumor treatment

1. Introduction

There are different methods for cancer treatment, such as chemotherapy and radiotherapy; however, side effects are a problem [1]. The hyperthermia system is one of the known methods used for cancerous tumor treatment without surgical operation by exposing the human body to heat. The hyperthermia system is effective while the heat is concentrated precisely on the tumor area so as to prevent damage to healthy tissues [1]-[5]. Currently, several types of hyperthermia are being operated: regional, local, and whole body. Tumor as a small treatment area is exposed to heat in local hyperthermia [1]-[2]. Radiofrequency, ultrasound, and microwave are known sources that produce heat [2]. Nowadays, microwaves are being operated in the hyperthermia system. Focusing these waves on the tumor area by a near-field lens may result in tumor malignant cells destruction because in the hyperthermic temperature range 43 ℃-47 ℃, heat is aggregated in cancerous cells, which causes necrosis due to low blood flow, while heat is dissipated in normal tissues, which maintain healthy cells safety [6]-[7].

In previous studies, microstrip-based Near-Field Focused (NFF) antennas have been used in hyperthermia systems [7]-[10]. In this paper, a dielectric lens is proposed for near-field applications in hyperthermia system for cancerous

Copyright ©2022 Behrooz Haghshenas-Kashani, et al.
DOI: https://doi.org/10.37256/est.3220221434
This is an open-access article distributed under a CC BY license
(Creative Commons Attribution 4.0 International License)
https://creativecommons.org/licenses/by/4.0/

tumor treatment, according to the idea of dividing flat lenses into different regions and devoting an exclusive constant to each zone [11]-[12], which reveals its novelty. Whereas dielectric lenses have been used primarily in far-field applications such as antenna and radar systems in the microwave frequency region already [13]-[17]. These lenses have the main advantage of being operated in wide bandwidth [18]. The simplicity of being integrated into the system and low profile are the other advantages of flat lenses [11]-[12]. The presented lens in this paper is also totally dielectric and no metallic layers are included, hence ohmic losses and mutual coupling would be predicted lower and subsequently, no surface current would be generated in the lens [15]. In this regard, a comparison between various methods which have been implemented in hyperthermia application and the proposed lens in this paper is presented in Table 1.

Table 1. The comparison table between the previously designed lenses for hyperthermia applications and the proposed method

Antenna type	Frequency	Methodology	Specific application	Ref.
Symmetric compact microwave radiator	433 MHz	Microstrip-based By reducing the size of radiator	Treatment of superficial tumors	[7]
Near-field microstrip-planar antenna	2.4 GHz	Microstrip-based By applying a proper phase shift to the elements, by selecting the accurate electrical length of the feedlines	Control the growth of hydatid cyst	[8]
Hexagonal focused array	433 MHz	Microstrip-based By optimizing the power transmission efficiency	Microwave hyperthermia	[9]
Near-field transmit-array lens antenna configuration	915 MHz	Microstrip-based Summation of EM energy by compensating for the phase delays for different path lengths from each elementary cell of the lens	Treatment of superficial tumors	[10]
Focused converging dielectric lens	2450 MHz	Dielectric-based By increasing the lens diameter	Hyperthermia application	[19]
A diverging dielectric lens attached to the dielectric rod antenna	8 GHz	Dielectric-based By adjusting the beam size of the lens	Treatment of different tumor sizes	[20]
Our proposed wideband dielectric near-field lens	2.4 GHz	Dielectric-based By dedicating exclusive dielectric constants to each region of a dielectric lens that has been divided into several zones	Treatment of superficial tumors	-

The main objective of this paper is to present the design of two different dielectric lenses in accordance with the location of the tumor in the human body: Type "1" for superficial tumors and type "2" for deep-seated tumors. Based on the dielectric constant distribution on the lens, the heat deposition would have occurred in the treatment target, which presents a noninvasive modality in tumor cell destruction. To evaluate the efficiency of the proposed hyperthermia system, the Specific Absorption Rate (SAR) and Effective Treatment Area (ETA) principles were used as indices [7]. The hyperthermia system is efficient when SAR distribution on phantom increases and ETA becomes concentrated compared to lens-free operation. The simulation setup in the hyperthermia system consists of an electromagnetic wave radiating antenna, a dielectric lens, and a one-layered phantom that simulates the muscle tissue of the human body. The excitation current amplitude for the dipole antenna as the radiating antenna is 0.3 A and its directivity is 2.293 dBi.

2. Design method of dielectric near-field lens

A flat circular one-layer lens including 13 concentric regions will be designed in accordance with Figure 1 so that Electromagnetic (EM) waves passing through the lens are focused on a spot (as a focal point) that is 20 cm from the lens surface. Each zone of the lens shall consist of exclusive dielectric constants. The magnetic permeability for all zones is determined by 1 and then the lens's thickness and diameter are specified as 3 cm and 25 cm, respectively.

Some requirements should be considered to design the dielectric lens, which will be followed. Initially, the phantom and antenna should be close together to minimize Distance-Related Losses (DRL) [21]. Then, the phantom and antenna should be far from each other in order to minimize Mismatch Losses (ML) [21]. Finally, following the equation $\theta = tg^{-1}\left(\frac{D/2}{d_1}\right)$, D and d_1 should be specified in such a way that the resulting θ is smaller than about 30°, where θ is the angle between the incident wave to the lens and horizontal axis, D represents lens diameter and d_1 is the distance between antenna and center zone of the lens.

2.1 *Design method of dielectric near-field lens for superficial tumors*

Figure 2(a) clarifies the strategy of one-layered lens design for the hyperthermia system, which includes a dipole antenna as a radiator producing EM waves, a dielectric near-field lens, and a proposed phantom for superficial tumors inside the human body.

Where d_1 is the distance between the radiator and center zone of the lens surface, d_2 is lens thickness and d_3 is the distance between the focal point and the lens surface's center zone. r_{N1} is also defined as the distance between the radiator and the nth zone of the lens and r_{N2} is specified as the distance between the nth zone of the lens and the focal point.

Dielectric constants for each lens zone will be determined based on (1), whereas the equation is independent of frequency.

$$k_0(d_1 + d_3) + k_0 d_2\sqrt{\varepsilon_{r1}} = k_0(r_{N1} + r_{N2}) + k_0 d_2\sqrt{\varepsilon_{rN}} \quad (1)$$

Where k_0 is wavenumber in air. Based on (1), terms of $k_0(d_1 + d_3) + k_0 d_2\sqrt{\varepsilon_{r1}}$ and $k_0(r_{N1} + r_{N2}) + k_0 d_2\sqrt{\varepsilon_{rN}}$ should be equivalent to ensure that EM waves passing through the dielectric lens are equiphase at the focal point that contributes to heat deposition. Consequently, focusing on the operation is achieved by choosing a suitable dielectric constant distribution on different regions to satisfy (1) that compensates for phase differences resulting from the distance of each zone from the desired spot. Hence, the dielectric constant of the highest region (ε_{rN}) has the lowest value, which has been selected "1.1" to obtain impedance matching of the lens and the surrounding environment. Subsequently, the dielectric constant of the center region (ε_{r1}) has the highest value. Note that although a higher dielectric ratio of the center regions would lead to reflection and mismatch, this occurs more around the central areas of the lens, and the value of the mismatch and reflection is negligible compared to the range of the EM waves passing through the lens. The resulted dielectric constants for each zone of the type "1" lens are listed in Table 2.

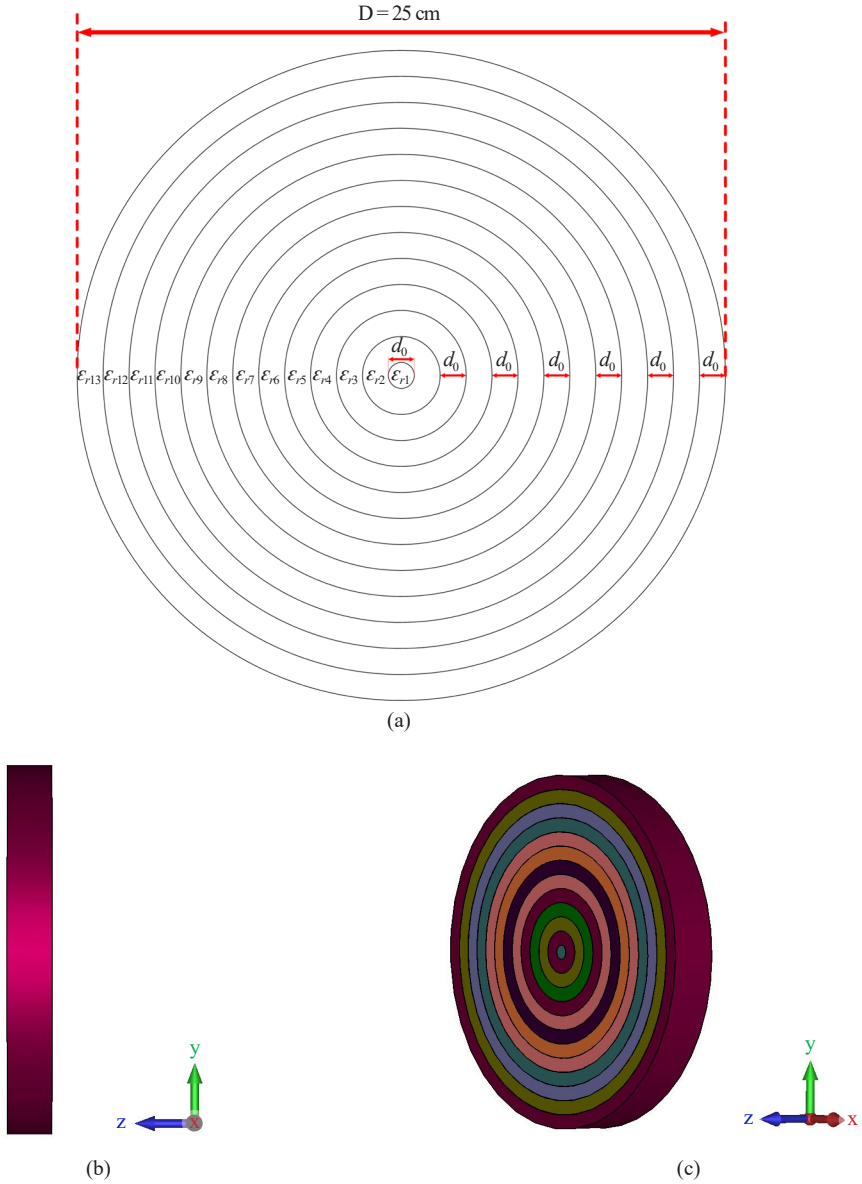

Figure 1. (a) Top view of one-layered circular regional dielectric lens (where d_0 is 1cm), (b) The side view of the dielectric lens, (c) The 3D view of the dielectric lens

2.2 *Design method of dielectric near-field lens for deep-seated tumors*

Unlike conventional designs for superficial tumors in the human body (Figure 2(a)), a new design is investigated for a deep-seated tumor that is located at 2 cm inside the phantom based on Figure 2(b). Dielectric constants of the lens for deep-seated tumors will be determined according to (2) when ε_{rbody} is 52.67 based on Table 3 and the dielectric constant of the highest region (ε_{rN}) has been specified as "1.1" same as the type "1" lens design.

$$k_0(d_1+d_3)+k_0d_2\sqrt{\varepsilon_{r1}}+k_0d_4\sqrt{\varepsilon_{rbody}}=k_0(r_{N1}+r_{N2})+k_0d_2\sqrt{\varepsilon_{rN}}+k_0r_{N3}\sqrt{\varepsilon_{rbody}} \quad (2)$$

Where

$$r_{N2}=\sqrt{d_3^2+(h_0-h)^2},\ r_{N3}=\sqrt{d_4^2+h^2}\ \text{ and }\ h=\frac{d_4h_0}{d_4+d_3\sqrt{\varepsilon_{rbody}}} \tag{3}$$

Where d_3 is the distance between the focal point and center zone of the lens surface and d_4 is the distance between the phantom surface and the focal point. r_{N2}, r_{N3}, and h are also obtained based on (3). The calculated dielectric constants for each zone of the type "2" lens are presented in Table 2, In contrast, all dielectric constants of its zones have been decreased compared to dielectric constants of the type "1" lens.

Table 2. The dielectric constants for each zone of the designed circular one-layered dielectric lens for superficial and deep-seated tumors

Zone	Dielectric constants (Type "1")	Dielectric constants (Type "2")
1	10.58	10.49
2	10.49	10.38
3	10.19	10.09
4	9.65	9.56
5	8.96	8.88
6	8.1	8.033
7	7.11	7.056
8	6.06	6.027
9	4.95	4.912
10	3.86	3.83
11	2.82	2.797
12	1.87	1.868
13	1.1	1.1

Table 3. EM features of the muscle tissue at 2.4 GHz [8]

Tissue	Relative permeability	Conductivity (S/m)	Mass density (10^3 kg/m^3)
Muscle	52.67	1.77	1.04

It should be noted that all mentioned precise dielectric constants in Table 2 may be achieved with an approximation in practice and subsequently, the practical results will differ from the theoretical ones briefly. Hence, based on simulation results, it has been observed that random changes of 3%, 5%, 10%, and 15% in values of calculated dielectric constants have resulted in maximum changes of 1%, 2%, 5%, and 15%, respectively, in SAR value distribution on the phantom, which demonstrates the level of SAR sensitivity to the permittivity values. Methods such as material drilling may be applied in order to fabricate and manufacture a flat inhomogeneous lens so that holes with different diameters are drilled on a plate form that realizes a non-uniform refractive index [22]-[26].

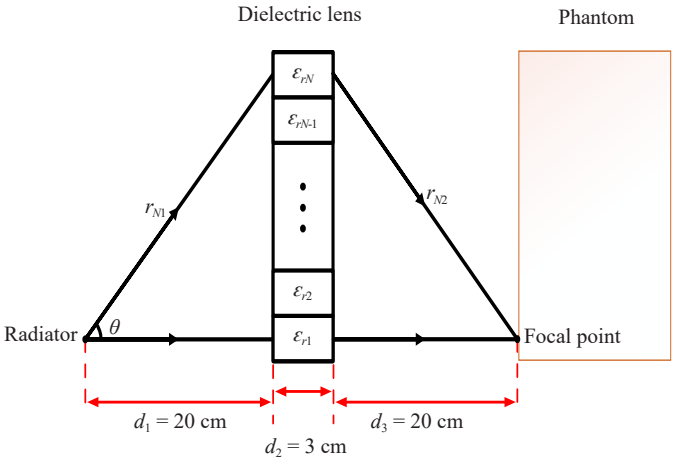

(a)

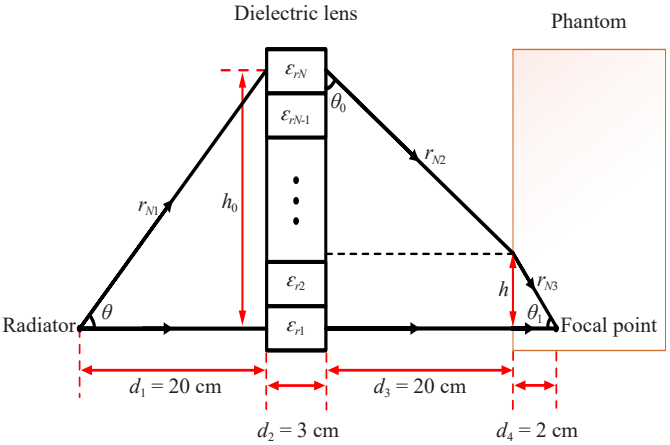

(b)

Figure 2. The strategy of dielectric near-field lens design (a) for a superficial tumor and (b) for a deep-seated tumor

3. Simulation results

The behavior of EM waves passing through the dielectric lens and being focused inside the phantom is investigated. Initially, the lens efficiency versus the frequency is shown in Figure 3. It is determined by the ratio of the power passing through the desired surface to the input power to the lens [27]. As shown in Figure 3, the highest efficiency occurs at 2.4 GHz, which would be about 66%. Furthermore, it is indicated that the efficiency fluctuates between 40% and 66% when the frequency increases from 2 to 2.8 GHz. In order to choose the proper frequency for simulating the proposed hyperthermia system, 2.45 GHz would be the highest allowable frequency for medical applications [6]. Hence, 2.4 GHz has been selected for the sake of the requirement for an optimal and efficient absorbed power density on the phantom (Considering the electrical properties of the phantom). This frequency will bring about the highest absorbed power on the treatment target, as observed in Figure 4. SAR values in different frequencies are achieved when the distance between the lens and phantom is 14 cm.

It should notice that the SAR value distribution on the phantom relies on the radiation antenna's input power. The input power is adjustable so that by changing the excitation current amplitude from 0.3 A to 1 A, 0.5 A, 0.4 A, and 1 mA SAR values at 2.4 GHz is changed to 12.17 W/kg, 3.043 W/kg, 1.947 W/kg, and 12.17e-6 W/kg, respectively, which reveals there is a direct relationship between the SAR distribution and current amplitude. Nevertheless, the main goal of the lens design in a hyperthermia system is determined when SAR and ETA distribution is improved and optimized

compared to lens-free operation to impress tumor cells. SAR value 1.095 W/kg is according to the averaging mass of 1 g for phantom, which meets the SAR limits of IEEE (1.6 W/kg for any 1 g of tissue [28]). The entire structure was simulated using the computer simulation technology microwave studio (CST MWS) [29]. All results are also depicted at 2.4 GHz based on the simulation setup of the presented hyperthermia system, which includes a radiator, lens, and a phantom, as featured in Figure 5. Where d_5, as the distance between the phantom location and lens surface, is changed between 14 cm and 20 cm to specify the desired distance. SAR distribution on the phantom is also displayed at points where the maximum SAR distribution has occurred.

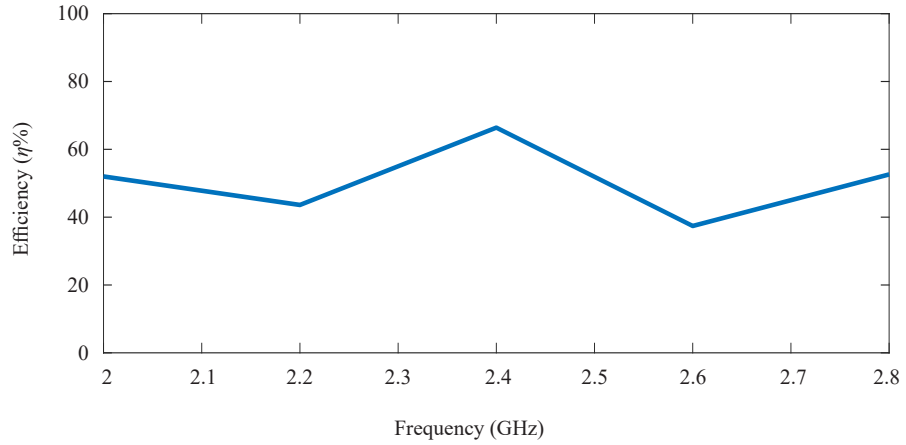

Figure 3. Lens efficiency versus frequency

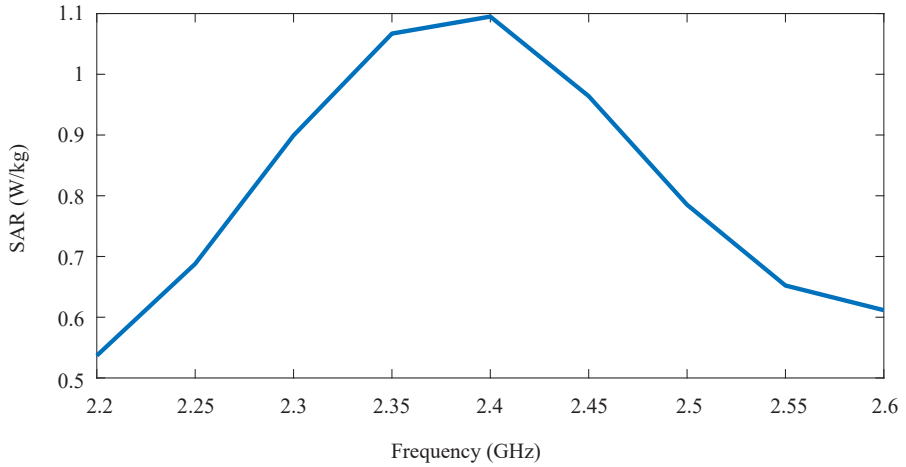

Figure 4. SAR values on a phantom that is achieved by type "1" lens operation at different frequencies

3.1 *Simulation results of designed lens for superficial tumor*

The E-field distribution and the power distribution in the free space (without phantom) and the E-field distribution on the phantom surface caused by the type "1" lens at 2.4 GHz are depicted in Figure 6, all of which represent the concentration of the dielectric lens in the near-field region. Moreover, The SAR caused on the phantom containing only the muscle layer by the lens is illustrated in Figure 7, where the EM features of the phantom have been listed previously in Table 3. As shown in Figure 6, Figure 7, and Table 4, the maximum E-field, SAR distribution, and the desired ETA

have occurred on a phantom that is 14 cm apart from the lens surface, at a depth of 0.072 cm inside the phantom, while the focal point has been designed at a distance of 20 cm. In this regard, Hanson also demonstrated that the peak of the E-Feild and subsequently the absorbed power peak will not be precisely on the focal point, it will befall in a spot between the focal point and lens surface due to the 1/r effect, which is the field-dissipating factor in the near-field area [30]. The penetration depth is illustrated in Figure 8, in which a -3 dB area in the Z-axis direction has occurred at a depth of 1.25 cm inside the phantom. Table 4 and Figure 8 illustrate that the type "1" proposed lens could be used for treating tumors located at a maximum depth of 1.25 cm inside the human body with an area of around 55.97 × 55.97 mm^2. All the above dimensions have been found at the points where the -3 dB of the power resulted.

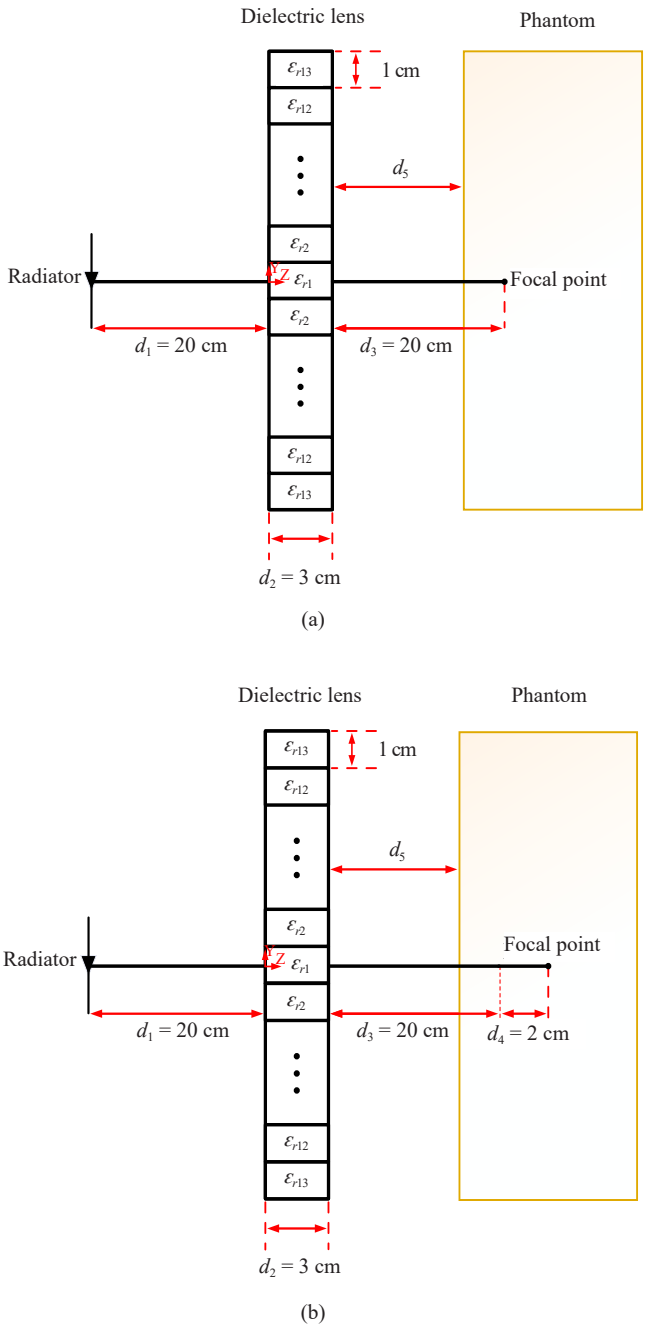

Figure 5. Simulation setup of the presented hyperthermia system, (a) for a superficial tumor, (b) for a deep-seated tumor

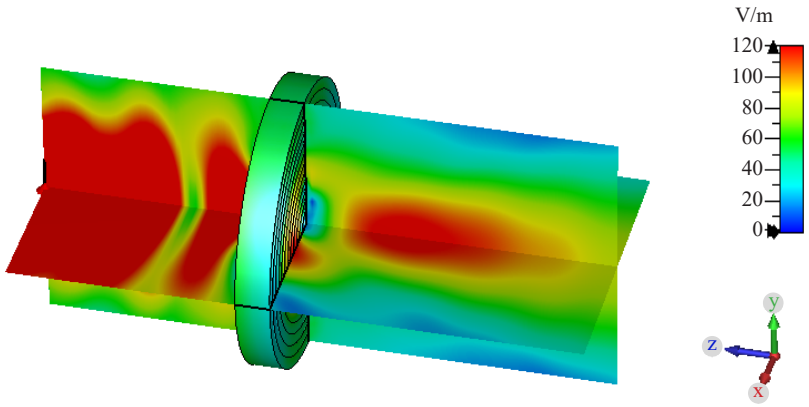

(a)

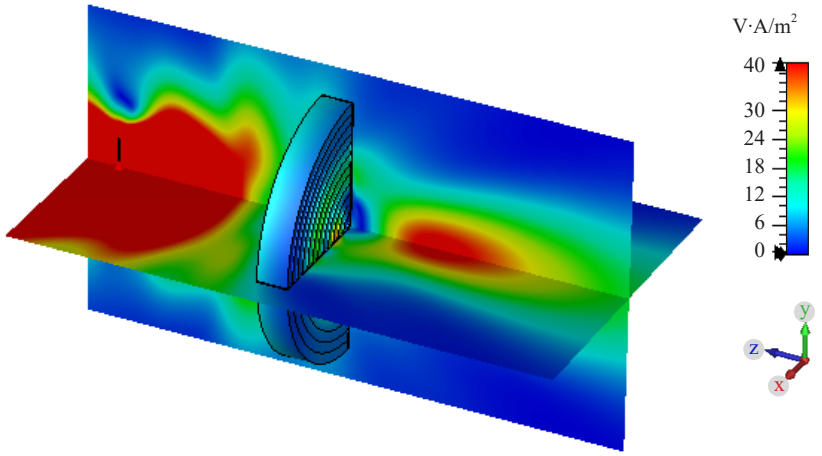

(b)

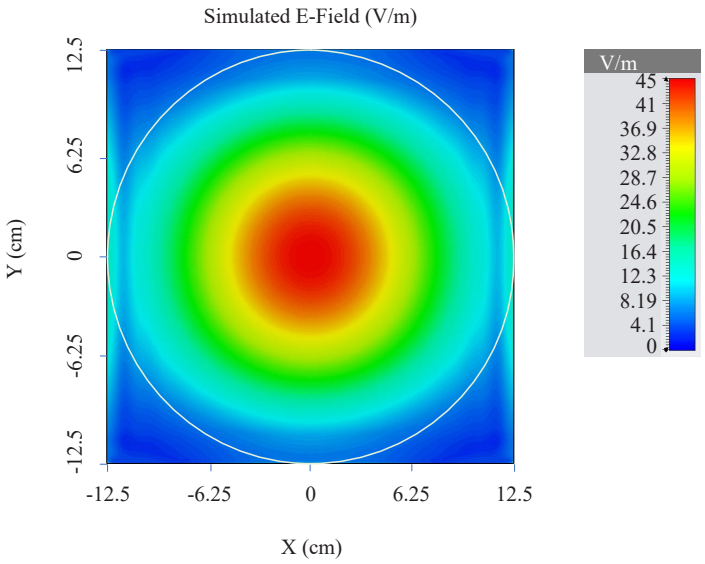

(c)

Figure 6. (a) Simulated E-Field distribution in the free space, (b) Simulated power distribution in the free space, (c) Simulated E-Field distribution on the phantom surface when d_5 is 14 cm

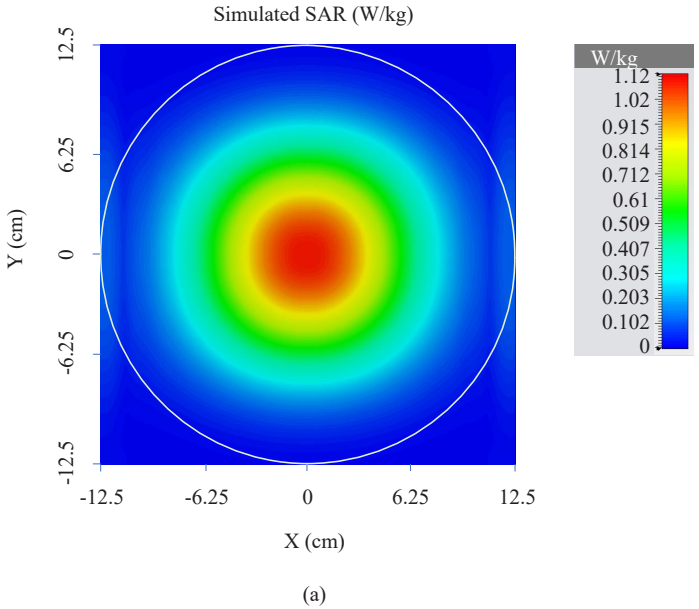

(a)

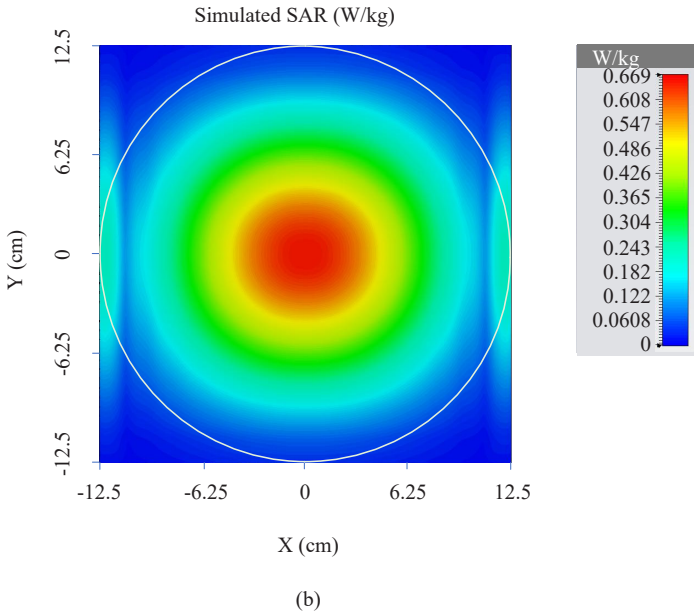

(b)

Figure 7. SAR distribution on the phantom for a superficial tumor (a) when d_5 is 14 cm and (b) when d_5 is 20 cm

Table 4. SAR values and -3 dB spot area on the phantom surface based on the designed lens for superficial tumor

d_5	Power loss density (W/m^3)	SAR (W/kg)	-3 dB spot area on the xy plane
14 cm	1680	1.095	55.97 × 55.97 mm^2
20 cm	999.6	0.6548	66.5 × 66.5 mm^2

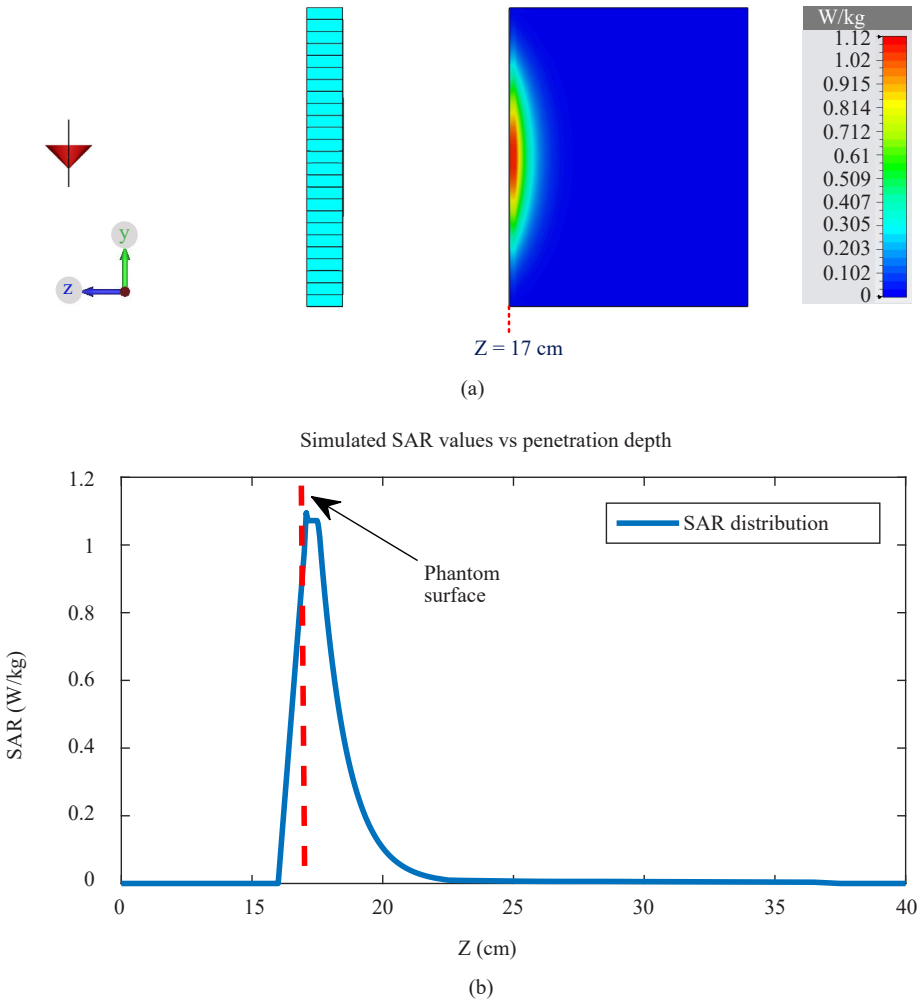

Figure 8. Penetration depth in the phantom for type "1" lens, when d_5 is 14 cm, (a) y-z view, (b) Cartesian coordination system

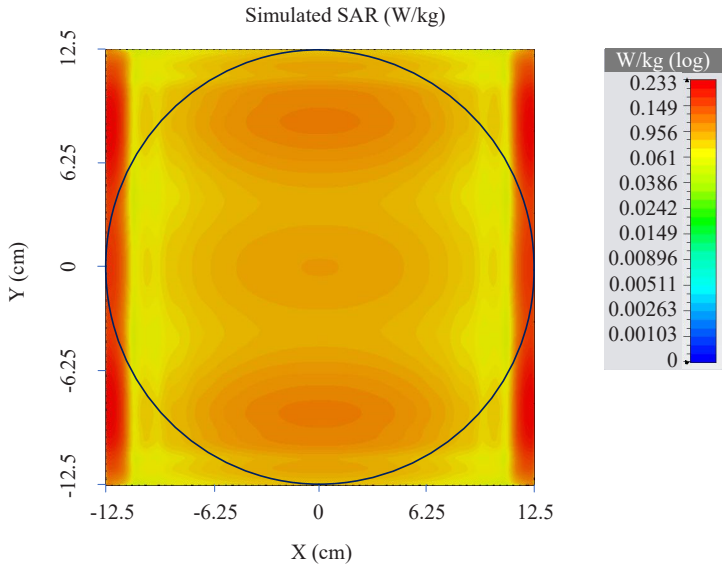

Figure 9. SAR distribution on a phantom in lens-free operation

In order to assess the designed lens efficiency, it should be compared with a lens-free operation. Remarkable differences between SAR distribution and ETA caused by lens-free operation and then type "1" lens can be detected because, in lens-free operation, SAR distribution on the phantom has decreased remarkably and reached its minimum value of 0.233 (W/Kg) and ETA has been spread over a wide area, as shown in Figure 9. Therefore, the high efficiency of the designed lens in superficial tumor treatment is comprehensible, based on the resulting SAR and ETA distributions.

3.2 *Simulation results of designed lens for deep-seated tumors*

Regarding the simulation results, SAR of 1.108 (W/kg) and 0.6629 (W/kg) is achieved by the designed lens for deep-seated tumors, where the phantom is located at 14 cm and 20 cm, respectively, apart from the lens surface. Although the SAR value distribution caused by the type "2" lens has been improved, there is no considerable difference compared to the SAR and ETA distribution resulting from the type "1" lens. The penetration depth also has not been changed where SAR_{max} (-3 dB) has happened still at a depth of 1.25 cm inside the phantom like the type "1" lens.

4. Conclusion

In this paper, unlike the previous microstrip-based designed lenses for hyperthermia applications, a new design for near-field lenses has been presented based on dedicating exclusive dielectric constants to each region of a dielectric lens divided into several zones. Two different designs for the dielectric near-field lenses that operate at 2.4 GHz have been proposed for tumor treatment, according to the tumor's location in the human body. As an index, a designed lens in the hyperthermia system is effective when EM waves are concentrated precisely in the desired target leading to heat accumulation during a defined time. As shown in the results, the proposed lens efficiency for the superficial tumor is considerable because SAR distribution has experienced an increase of about 4.5-time and ETA has been focused noticeably in comparison to the lens-free operation, nonetheless designed lens efficiency for deep-seated tumors was not remarkable because it was supposed that the maximum SAR would have happened at a depth of 2 cm inside the phantom in keeping with type "2" design, whereas the result was approximately similar to type "1" design. Nevertheless, the designed lens for superficial tumors may be operated on the hyperthermia system as a result of the ever-increasing necessity of the methods for cancer treatment to destroy the cancerous tumors.

Conflict of interest

The authors declare that there is no personal or organizational conflict of interest with this work.

References

[1] M. Aldhaeebi, M. Alzabidi, and I. Elshafiey, "Optimization of UWB antenna array for hyperthermia treatment of brain tumor," 2013 Saudi International Electronics, Communications and Photonics Conference, Fira, 2013, pp. 1-6.

[2] H. Younesiraad, M. Bemani, and S. Nikmehr, "A dual-band slotted square ring patch qntenna for local hyperthermia applications," *Progress In Electromagnetics Research Letters*, vol. 71, pp. 97-102, 2017.

[3] Y. Xiao, L. Wu, S. S. Peng, and Z. L. Xiao, "Single-layer metasurface focusing lens for medical applications," 2019 IEEE MTT-S International Microwave Biomedical Conference (IMBioC), 2019, pp. 1-3.

[4] N. A. Jaffar, N. Buniyamin, and K. Lias, "An overview of available metamaterial-based antenna for non-invasive hyperthermia cancer treatment," *Indonesian Journal of Electrical Engineering and Computer Science*, vol. 14, no. 2, pp. 697-705, 2019.

[5] N. Sharma, H. S. Singh, R. Khanna, A. Kaur, and M. Agarwal, "Development of deeply focused microwave lens applicator for efficient hyperthermia treatment," *Optik-International Journal for Light and Electron Optics*, vol. 259, no. 2013, pp. 168946, 2022.

[6] M. Melek and A. P. Anderson, "Theoretical studies of localised tumour heating using focused microwave arrays," *IEE Proceedings F-Communications, Radar and Signal Processing*, vol. 127, no. 4, pp. 319-321, 1980.

[7] W. C. Choi, K. J. Kim, J. Kim, and Y. J. Yoon, "Compact microwave radiator for improving heating uniformity in hyperthermia system," *IEEE Antennas and Wireless Propagation Letters*, vol. 13, pp. 1345-1348, 2014.
[8] F. Tofigh, J. Nourinia, M. Azarmanesh, and K. M. Khazaei, "Near-field focused array microstrip planar antenna for medical applications," *IEEE Antennas and Wireless Propagation Letters*, vol. 13, pp. 951-954, 2014.
[9] X. He, W. Geyi, and S. Wang, "A hexagonal focused array for microwave hyperthermia: Optimal design and experiment," *EEE Antennas and Wireless Propagation Letters*, vol. 15, pp. 56-59, 2016.
[10] W. C. Choi, S. Lim, and Y. J. Yoon, "Design of noninvasive hyperthermia system using transmit-array lens antenna configuration," *IEEE Antennas and Wireless Propagation Letters*, vol. 15, pp. 857-860, 2016.
[11] Y. Zhang, R. Mittra, and W. Hong, "A zoned two-layer flat lens design," 2011 International Workshop on Antenna Technology (iWAT), Hong Kong, 2011, pp. 412-415.
[12] P. Li and Y. L. Guan, "The design of two-layer flat lens," 2014 IEEE Workshop on Advanced Research and Technology in Industry Applications (WARTIA), Ottawa, ON, 2014, pp. 1108-1110.
[13] S. Ravishankar, "Analysis of shaped beam dielectric lens antennas for mobile broadband applications," IWAT 2005. IEEE International Workshop on Antenna Technology: Small Antennas and Novel Metamaterials, 2005, Singapore, 2005, pp. 539-542.
[14] Z. X. Wang and W. B. Dou, "Dielectric lens antennas designed for millimeter wave application," 2006 Joint 31st International Conference on Infrared Millimeter Waves and 14th International Conference on Teraherz Electronics, Shanghai, 2006, pp. 376-376.
[15] B. Panzner, A. Joestingmeier, and A. Omar, "Ka-Band dielectric lens antenna for resolution enhancement of a GPR," 2008 8th International Symposium on Antennas, Propagation and EM Theory, Kunming, 2008, pp. 31-34.
[16] M. K. T. Al-Nuaimi, W. Hong, and Y. Zhang, "Design of high-directivity compact-size conical horn lens antenna," *IEEE Antennas and Wireless Propagation Letters*, vol. 13, pp. 467-470, 2014.
[17] M. Imbert, J. Romeu, M. Baquero-Escudero, M. Martinez-Ingles, J. Molina-Garcia-Pardo, and L. Jofre, "Assessment of LTCC-based dielectric flat lens antennas and switched-beam arrays for future 5G millimeter-wave communication systems," *IEEE Transactions on Antennas and Propagation*, vol. 65, no. 12, pp. 6453-6473, Dec. 2017.
[18] M. A. Al-Joumayly and N. Behdad, "Wideband planar microwave lenses using sub-wavelength spatial phase shifters," *IEEE Transactions on Antennas and Propagation*, vol. 59, no. 12, pp. 4542-4552, Dec. 2011.
[19] A. A. Rahman, K. Kamardin, and Y. Yamada, "Focal spot size evaluation of a gocused lens in human body," 2020 IEEE International RF and Microwave Conference (RFM), 2020, pp. 1-4.
[20] I. H. Uluer, M. J. Jaroszeski, and T. M. Weller, "Dielectric lens designs for antenna beam shaping in a subdermal tumor treatment device," 2021 IEEE MTT-S International Microwave Symposium (IMS), 2021, pp. 370-373.
[21] S. Curto, "Antenna development for radio frequency hyperthermia applications," Doctoral Thesis, Technological University Dublin, Dublin, 2010.
[22] B. Zhou, Y. Yang, H. Li, and T. J. Cui, "Beam-steering vivaldi antenna based on partial Luneburg lens constructed with composite materials," *Journal of Applied Physics*, vol. 110, no. 8, 084908, 2011.
[23] C. D. Gu, K. Yao, W. X. Lu, Y. Lai, H. Y. Chen, B. Hou, and X. Y. Jiang, "Experimental realization of a broadband conformal mapping lens for directional emission," *Applied Physics Letters*, vol. 100, no. 26, 261907, 2012.
[24] T. Driscoll, G. Lipworth, J. Hunt, N. Landy, N. Kundtz, D. N. Basov, and D. R. Smith, "Performance of a three-dimensional transformation-optical-flattened Lüneburg lens," *Optics Express*, vol. 20, no. 12, pp. 13262-13273, 2012.
[25] O. Lafond, M. Himdi, H. Merlet, and P. Lebars, "An active reconfigurable antenna at 60 GHz based on plate inhomogeneous lens and feeders," *IEEE Transactions on Antennas and Propagation*, vol. 61, no. 4, pp. 1672-1678, 2012.
[26] M. M. Taskhiri and M. K. Amirhosseini, "Design of a broadband hemispherical wave collimator lens using the ray inserting method," *Journal of the Optical Society of America A*, vol. 34, no. 7, pp. 1265-1271, 2017.
[27] W. Zhu and J. Li, "Experimental realization of ultra-compact high-efficiency metasurface Luneburg lenses for microwave applications," *Journal of Physics: Conference Series*, vol. 1461, no. 1, 012200, 2020.
[28] IEEE Standards for Safety Levels with Request to Human Exposure to Radiofrequency Electromagnetic Fields, 3kHz to 300GHz. IEEE Std. C95.1. 1999.
[29] CST STUDIO SUITE, Computer Simulation Technology AG, Available: www.cst.com [Accessed June 15, 2022].
[30] R. Hansen, "Focal region characteristics of focused array antennas," *IEEE Transactions on Antennas and Propagation*, vol. 33, no. 12, pp. 1328-1337, 1985.

Author biographies

Behrooz Haghshenas-Kashani was born in Kashan, Iran, in 1992. He received B.Sc. degree in electrical engineering from Shahid Beheshti University, Tehran, in 2016, the M.Sc. degree in electrical engineering from Iran University of Science and Technology (IUST), Tehran, Iran, in 2018. He is currently working as an electrical engineer at Canymes industrial and mining company.

Mohammad-Ali Damavandi was born in Hamedan, Iran, in 1986. He received the B.Sc. and M.Sc. degrees in electrical engineering from the Islamic Azad University Central Tehran Branch and Shahid Beheshti University, Tehran, Iran, respectively in 2009 and 2016. He is currently a Ph.D. student at the Iran University of Science and Technology (IUST), Tehran, Iran.

Mohammad Khalaj-Amirhosseini was born in Tehran, Iran in 1969. He received the B.Sc., M.Sc., and Ph.D. degrees in Electrical Engineering from the Iran University of Science and Technology (IUST), Tehran, in 1992, 1994, and 1998 respectively. He is currently a professor in the school of electrical engineering, IUST.